Effective Elasticity of Functionally Graded Composites: A Micromechanics Framework with Particle Interactions

H.M. Yin[a], G. H. Paulino[a], and L.Z. Sun[b]

[a]*Department of Civil and Environmental Engineering*
University of Illinois at Urbana-Champaign, Urbana, IL 61801
[b]*Department of Civil and Environmental Engineering*
University of California, Irvine, CA 92697

Abstract. The present paper aims to develop a micromechanics-based effective elastic model of functionally graded composites. At the macroscopic scale, effective material properties of the composites are uniform in the same graded layer while gradually changing along the grading direction. Microstructurally, infinite particles are randomly dispersed in the matrix with gradual transitions. Particles are assumed to be spherical and nonintersecting. They are perfectly bonded with the matrix. A micromechanical framework is proposed to investigate effective mechanical properties along the grading direction. Within the context of the representative volume element (RVE), the effect of pair-wise interactions between particles is taken into account for the local stress and strain fields by using the modified Green's function method. Homogenization of the local field renders relations between the averaged strain, strain gradient and external loading. The effective elastic modulus tensor of the functionally graded composites is further constructed by numerical integration. The model prediction is compared with available experimental data.

Keywords: Functionally graded composites; Micromechanical modeling; Effective elasticity; Stress and strain; Homogenization

INTRODUCTION

Functionally graded materials (FGMs) have attracted much attention from engineers and researchers due to their unique thermomechanical performance [1, 2]. Several FGMs are manufactured by two phases of materials with different properties. Since the volume fraction of each phase gradually varies in the gradation direction, the effective properties of FGMs change in this direction. While FGMs have been designed and fabricated by diverse methods to achieve unique microstructures, very limited analytical investigations are available to tackle the spatial variation of microstructure [3]. Conventional composite models such as the Mori-Tanaka method [4] and the self-consistent method [5, 6] are directly applied to estimate the effective elastic responses of FGMs [2]. Because they were originally developed for homogeneous mixtures with constant particle concentration, those models are not able to capture the material gradient nature of FGMs. Furthermore, no direct interactions between particles are taken into consideration [7].

Experimental observations [2, 8] show that the typical microstructure of FGMs, illustrated in Fig. 1(a) towards the gradation direction, contains a particle-matrix zone

CP973, *Multiscale and Functionally Graded Materials 2006*
edited by G. H. Paulino, M.-J. Pindera, R. H. Dodds, Jr., F. A. Rochinha, E. V. Dave, and L. Chen
© 2008 American Institute of Physics 978-0-7354-0492-2/08/$23.00

Downloaded 18 Nov 2009 to 192.17.145.10. Redistribution subject to AIP license or copyright; see http://proceedings.aip.org/proceedings/cpcr.jsp

with discrete particles filled in continuous matrix, followed by a skeletal transition zone in which the particle and matrix phases cannot be well defined because the two phases are interpenetrated into each other as a connected network. The transition zone is further followed by another particle-matrix zone with interchanged phases of particle and matrix. Hirano et al. [8] applied the fuzzy logic approach to estimate the effective elastic behavior in the transition zone by using a transition function to combine the two solutions obtained from the particle-matrix zones. Reiter and Dvorak [9] also adopted the transition functions combined with the Mori-Tanaka model in the particle-matrix zone and self-consistent model in the skeletal transition zone.

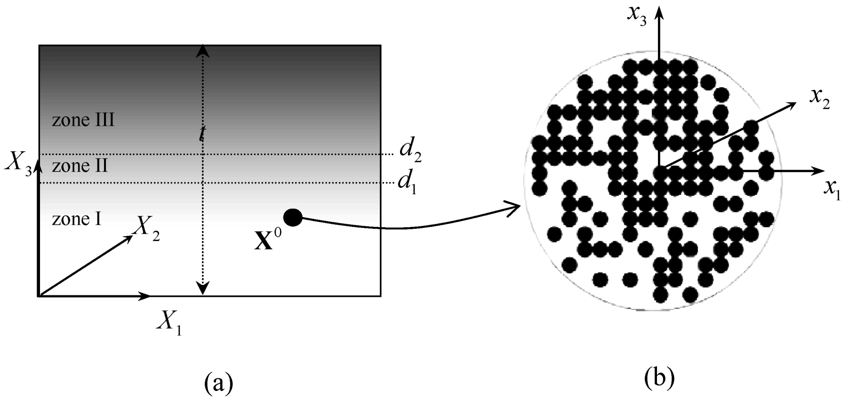

FIGURE 1. Schematic illustration of a two-phase FGM sample: (a) three zones in macroscopic scale and (b) RVE in the microscopic scale.

The above-mentioned FGMs models did not include the local interactions between particles, so they could not take into account the graded particle distribution for FGMs. Some studies have suggested the need for higher order theory in the modeling of FGMs [3, 10-12]. In this paper a micromechanical framework is proposed to investigate the effective elastic behavior of FGMs. Given a uniform loading on the top and bottom boundaries of FGMs, a microscopic representative volume element (RVE) is constructed to reflect the microstructure of the particle-matrix zone in FGMs (Fig. 1(b)), and averaged strains in particles are derived by integrating pair-wise interaction contributions of all particles. Finally the effective stress and strain fields can be solved as differentiable functions in the gradation direction.

FORMULATION

Let us consider a typical FGM microstructure (Fig. 1) containing two phases A and B with isotropic elastic stiffness $\mathbf{C}^A$ and $\mathbf{C}^B$, respectively. The global coordinate system of the FGM is denoted by (X_1, X_2, X_3) with X_3 being the continuous gradation direction. The overall grading thickness of the FGM is t. The volume fraction of phase A or B (for convenience, we use ϕ to denote the volume fraction of phase A) is gradually changed in the gradation direction X_3. Microscopically, the particle and the

Downloaded 18 Nov 2009 to 192.17.145.10. Redistribution subject to AIP license or copyright; see http://proceedings.aip.org/proceedings/cpcr.jsp

matrix zones could be well defined when ϕ is close to 0 or 1 [e.g., Zone I and Zone III in Fig. 1(b)]. However, a skeletal transition zone (Zone II) normally exists in middle area (e.g., $d_1 < X_3 < d_2$) in which it is difficult to identify the particle or matrix phase.

Apply a uniform stress tensor $\boldsymbol{\sigma}^0$ on the FGM X_3 boundary. Based on the equilibrium condition, the averaged stress in any $X_1 - X_2$ layer is still $\boldsymbol{\sigma}^0$, so we can write:

$$\boldsymbol{\sigma}^0 = \bar{\mathbf{C}}(X_3) : \langle \boldsymbol{\varepsilon} \rangle (X_3) \tag{1}$$

where $\bar{\mathbf{C}}$ is the effective elasticity of that layer. The averaged strain and stress in the $X_1 - X_2$ layer can be further written as

$$\langle \boldsymbol{\varepsilon} \rangle (X_3) = \phi(X_3) \langle \boldsymbol{\varepsilon} \rangle^A (X_3) + \left[1 - \phi(X_3)\right] \langle \boldsymbol{\varepsilon} \rangle^B (X_3). \tag{2}$$

and

$$\boldsymbol{\sigma}^0 = \phi(X_3) \mathbf{C}^A : \langle \boldsymbol{\varepsilon} \rangle^A (X_3) + \left[1 - \phi(X_3)\right] \mathbf{C}^B : \langle \boldsymbol{\varepsilon} \rangle^B (X_3). \tag{3}$$

For any macroscopic material point $\mathbf{X}^0$ [Fig. 1(a)] in the range of $0 \le X_3 \le d_1$ (Zone I), the corresponding microstructural RVE [Fig. 1(b)] contains a number of micro-particles of the phase A embedded in a continuous matrix of the phase B so that the overall volume fraction of particle phase A and its gradient should be consistent with the macroscopic counterparts $\phi(X_3^0)$ and $d\phi / dX_3 |_{X_3 = X_3^0}$. The microscopic coordinate system (x_1, x_2, and x_3) is constructed with the origin corresponding to $\mathbf{X}^0$. The whole RVE domain is denoted as D and the i^{th} micro-particle $(i = 1, 2, 3, \cdots, \infty)$ domain is denoted as Ω_i centered at $\mathbf{x}^i$. The particle centered at the origin is assumed and denoted as Ω_0.

By considering the pair-wise particle interactions from all other particles, the averaged strain in the central particle Ω_0 can be written in two parts: the elastic-mismatch interaction between the central particle and the matrix and the pair-wise interaction between the central particle and other particles [11]:

$$\langle \boldsymbol{\varepsilon} \rangle^A (\mathbf{0}) = (\mathbf{I} - \mathbf{P}_0 \cdot \Delta\mathbf{C})^{-1} : \langle \boldsymbol{\varepsilon} \rangle^B (0) + \sum_{i=1}^{\infty} \Delta\mathbf{C}^{-1} \cdot \mathbf{L}(\mathbf{0}, \mathbf{x}^i) \langle \boldsymbol{\varepsilon} \rangle^B (x_3^i), \tag{4}$$

where $\Delta\mathbf{C} = \mathbf{C}^A - \mathbf{C}^B$, $(P_0)_{ijkl} = [\delta_{ij}\delta_{kl} - (4 - 5\nu_0)(\delta_{ik}\delta_{jl} + \delta_{il}\delta_{jk})] / [30\mu_0(1 - \nu_0)]$, $\langle \boldsymbol{\varepsilon} \rangle^B (0)$ is the averaged matrix strain in the layer with $x_3 = 0$, $\langle \boldsymbol{\varepsilon} \rangle^B (x_3^i)$ is the averaged matrix strain tensor in the x_3^i-th layer, and $\mathbf{L}(\mathbf{0}, \mathbf{x}^i)$ describes the interaction of the particle centered at $\mathbf{x}^i$ on the averaged strain of the central particle. The pair-wise interaction tensor $\langle \mathbf{d} \rangle (\mathbf{0})$ [i.e., the second term of the right hand side of Eq. (4)] can be further integrated over all possible particle positions as:

$$\langle \mathbf{d} \rangle (\mathbf{0}) = \sum_{i=1}^{\infty} \Delta\mathbf{C}^{-1} \cdot \mathbf{L}(\mathbf{0}, \mathbf{x}^i) : \langle \boldsymbol{\varepsilon} \rangle^B (x_3^i) = \int_D P(\mathbf{x} | \mathbf{0}) \Delta\mathbf{C}^{-1} \cdot \mathbf{L}(\mathbf{0}, \mathbf{x}) : \langle \boldsymbol{\varepsilon} \rangle^B (x_3) \, d\mathbf{x}. \tag{5}$$

Downloaded 18 Nov 2009 to 192.17.145.10. Redistribution subject to AIP license or copyright; see http://proceedings.aip.org/proceedings/cpcr.jsp

For the FGM considered, since the micro-particles in RVE are distributed in a continuously increasing manner in the gradation direction, the particle density function is proposed as

$$P(\mathbf{x}\,|\,\mathbf{0}) = \frac{3g(x)}{4\pi a^3}\left[\phi\left(X_3^0\right) + e^{-x/\delta}\phi_{,3}\left(X_3^0\right)x_3\right] \tag{6}$$

where $g(x)$ is the radial distribution function of particles proposed by Percus and Yevick [13] to estimate the particle non-uniformity effect in the radial direction. The expression enclosed by square brackets is constructed on the basis that the averaged volume fraction of particle in the RVE is $\phi\left(X_3^0\right)$, the gradient of particle volume fraction is $\phi_{,3}\left(X_3^0\right)$, and in the far field the particle concentration must not be beyond the range of zero to the maximum particle concentration. Thus, an exponential function is introduced to attenuate the gradation term exponentially. The parameter δ, which controls the attenuating rate, will be determined under the condition that the maximum volume fraction of particles in the RVE should not be greater than the maximum volume fraction in particle-matrix zone. Those particles in the neighboring domain of the central particle should contribute the majority part for the averaged strain of the central particle.

Similarly to Ju and Chen [7], the Taylor expansion of $\langle\boldsymbol{\varepsilon}\rangle^B(x_3)$ is applied to analytically integrate Eq. (5). It is noted that the average strain $\langle\boldsymbol{\varepsilon}\rangle^B(x_3)$ varies along the grading direction. It is differentiable and bounded, and thus is approximated by the Taylor expansion. In the chosen RVE, the elastic interaction between the central particle and the particles far away from it is negligible; only the particles in the close neighborhood of the central particle may have noticeable interaction on the central particle. As a first order approximation, we truncate the Taylor expansion of $\langle\boldsymbol{\varepsilon}\rangle^B(x_3)$ to linear term in terms of x_3 so that Eq. (5) can be analytically integrated and rewritten as

$$\langle\mathbf{d}\rangle(\mathbf{0}) = \phi\left(X_3^0\right)\Delta\mathbf{C}^{-1}\cdot\mathbf{D}(0):\langle\boldsymbol{\varepsilon}\rangle^B(0) + \phi_{,3}\left(X_3^0\right)\Delta\mathbf{C}^{-1}\cdot\mathbf{F}(0):\langle\boldsymbol{\varepsilon}\rangle^B_{,3}(0) \tag{7}$$

where

$$\mathbf{D} = \int_D \frac{3g(x)}{4\pi a^3}\mathbf{L}(\mathbf{0},\mathbf{x})\,d\mathbf{x};\ \mathbf{F} = \int_D e^{-x/\delta}\frac{3g(x)}{4\pi a^3}\mathbf{L}(\mathbf{0},\mathbf{x})\,x_3^2\,d\mathbf{x}. \tag{8}$$

Substituting Eq. (7) into Eq. (4) and recognizing that the origin of the local coordinates in the RVE corresponds to the global coordinate point $\mathbf{X}^0$ of FGM, we can obtain the averaged particle strain tensor in terms of the arbitrary material point X_3

$$\begin{aligned}\langle\boldsymbol{\varepsilon}\rangle^A(X_3) = {} & (\mathbf{I}-\mathbf{P}_0\cdot\Delta\mathbf{C})^{-1}:\langle\boldsymbol{\varepsilon}\rangle^B(X_3) + \phi(X_3)\Delta\mathbf{C}^{-1}\cdot\mathbf{D}(X_3):\langle\boldsymbol{\varepsilon}\rangle^B(X_3) \\ & + \phi_{,3}(X_3)\Delta\mathbf{C}^{-1}\cdot\mathbf{F}(X_3):\langle\boldsymbol{\varepsilon}\rangle^B_{,3}(X_3)\end{aligned}. \tag{9}$$

With the combination of Eqs. (3) and (9), the averaged particle strain tensor $\langle\boldsymbol{\varepsilon}\rangle^A(X_3)$ and the averaged matrix strain tensor $\langle\boldsymbol{\varepsilon}\rangle^B(X_3)$ in the FGM gradation

Downloaded 18 Nov 2009 to 192.17.145.10. Redistribution subject to AIP license or copyright; see http://proceedings.aip.org/proceedings/cpcr.jsp

direction X_3 can be solved in terms of the far-field stress $\boldsymbol{\sigma}^0$. Since Eq. (9) is a set of ordinary differential equations, we also need the appropriate boundary conditions. In the particle-matrix zone with $0 \le X_3 \le d_1$, the boundary at $X_3 = 0$ corresponds to the 100% matrix material (i.e., $\phi(0) = 0$). The corresponding boundary conditions can be proposed as

$$\langle \boldsymbol{\varepsilon} \rangle^B (0) = \mathbf{C}^{B^{-1}} : \boldsymbol{\sigma}^0 . \qquad (10)$$

Therefore, the averaged strain tensors in both phases can be numerically solved on the basis of standard backward Eulerian method. Similarly, in the other particle-matrix with the range of $d_2 \le X_3 \le t$ (zone III), we can also calculate the averaged strain fields by the switch of matrix and particle phases.

For the transition zone II ($d_1 < X_3 < d_2$), the particle and matrix phases cannot be well defined because the two phases are interpenetrated into each other as a connected network. As a consequence, the averaged elastic fields cannot explicitly be determined through the micromechanics framework. Similarly to Reiter and Dvorak [9], a phenomenological transition function is introduced as

$$f(X_3) = \left[1 - 2 \frac{\phi(X_3) - \phi(d_1)}{\phi(d_1) - \phi(d_2)} \right] \left[\frac{\phi(X_3) - \phi(d_2)}{\phi(d_1) - \phi(d_2)} \right]^2 \qquad (11)$$

so that the averaged strain of each phase (A or B) in the transition zone II can be approximated as a cubic Hermite function appropriately contributed by the averaged strain of the same phase (A or B) from two particle-matrix zones (zones I and III). Namely,

$$\langle \boldsymbol{\varepsilon} \rangle^{A \text{ or } B}_{zone-II} (X_3) = f(X_3) \langle \boldsymbol{\varepsilon} \rangle^{A \text{ or } B}_{zone-I} (X_3) + \left[1 - f(X_3) \right] \langle \boldsymbol{\varepsilon} \rangle^{A \text{ or } B}_{zone-III} (X_3) \qquad (12)$$

The overall averaged strain tensor at each layer in the transition zone can be further obtained from Eq. (2). It is noted that the proposed transition function makes the effective FGM elastic fields bounded, continuous, and differentiable.

RESULTS AND DISCUSSION

When a uniformly distributed stress is applied on the top and bottom boundaries of the FGM, the proposed model can be used to determine the averaged elastic fields as a function of X_3. Since two-phase FGMs are fabricated to gradually change material phases from one end to the other, the effective strain fields strongly depend on the individual performance of constituent phases. In the following simulation, the material selected is the C/SiC system (Reiter et al. [12]) with the carbon as phase A ($E_A = 28GPa, v_A = 0.3$) and the silicon carbide as phase B ($E_B = 320GPa, v_B = 0.3$). The volume fraction distribution function of silicon carbide is assumed as $\phi(X_3) = X_3 / t$ with the thickness of the FGM $t = 1$. The transition zone is taken from $\phi(d_1) = 48\%$ to $\phi(d_1) = 52\%$ to be consistent with FEM simulation [12].

Downloaded 18 Nov 2009 to 192.17.145.10. Redistribution subject to AIP license or copyright; see http://proceedings.aip.org/proceedings/cpcr.jsp

First we study the elastic fields of the FGM under a uniform shear $\sigma_{13} = 1.0MPa$ on the top and bottom boundary. Fig. 2(a) illustrates the overall averaged strain and compares the proposed model with the self-consistent method and finite element method (FEM) both performed by Reiter et al. [12]. It is shown that averaged shear stress on the carbon phase estimated by the current model is much closer to the numerical FEM results than the one estimated by the self-consistent method.

When the FGM is subjected to a uniform compression $\sigma_{33} = 1.0MPa$, we can also determine the averaged strain distribution as illustrated in Fig. 2(b). In the loading direction, the strain is negative; whereas it is positive in the direction normal to the loading. From these two figures we can see a continuous and differentiable jump in the transition zone. It can be predicted that a larger transition zone made during FGM fabrication is desirable to prevent the significant jump of effective elasticity when the elastic contrast ratio is big.

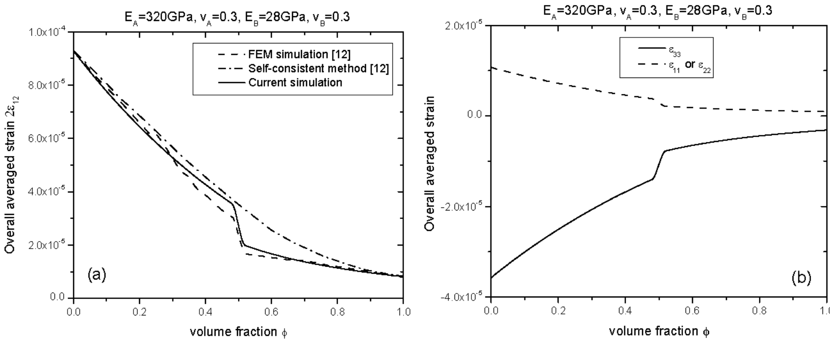

FIGURE 2. Schematic illustration of a two-phase FGM sample: (a) three zones in macroscopic scale and (b) RVE in the microscopic scale.

Due to a uniformly distributed stress applied on the FGM top and bottom boundaries, from the equilibrium condition the averaged stress can be easily obtained as the applied stress. Once we solve the averaged strain distribution in the gradation direction, we can further solve the elasticity distribution [11].

REFERENCES

1. Y. Miyamoto, W. A. Kaysser, B. H. Rabin, A. Kawasaki and R. G. Ford: Functionally graded materials: design, processing and applications (Kluwer Academic Publishers, 1999).
2. G. H. Paulino, Z. H. Jin and R. H. Dodds. In: B. Karihaloo and W. G. Knauss, editors. Comprehensive structural integrity, **2**, 607 (2003).
3. J. Aboudi, M.-J. Pindera and S. M. Arnold, *Composites Part B*, **30**, 777, (1999).
4. T. Mori and K. Tanaka, *Acta Metall.* **21**, 571 (1973).
5. R. Hill, *J. Mech. Phys. Solids*, **13**, 213 (1965).
6. B. Budiansky, *J. Mech. Phys. Solids,* **13**, 223 (1965).
7. J. W. Ju and T. M. Chen, *Acta Mech.* **103**, 123 (1994).
8. T. Hirano, J. Teraki and T. Yamada, *SMiRT 11 Transactions*, **SD1**, 49 (1991).
9. T. Reiter and G. J. Dvorak, *J. Mech. Phys. Solids*, **46**, 1655 (1998).
10. J. R. Zuiker and G. J. Dvorak, *Compos. Eng.* **4**, 19 (1994).
11. H. M. Yin, L. Z. Sun and G. H. Paulino, *Acta Mater.* **52**, 3535 (2004).
12. T. Reiter, G. J. Dvorak and V. Tvergaard, *J. Mech. Phys. Solids*, **45**, 1281 (1997).
13. J. K. Percus and G. J. Yevick, *Phys. Rev.* **110**, 1 (1958).

Downloaded 18 Nov 2009 to 192.17.145.10. Redistribution subject to AIP license or copyright; see http://proceedings.aip.org/proceedings/cpcr.jsp